Aquatic carbon concentrations and fluxes in a degraded blanket peatland with piping and pipe outlet blocking

Abstract

Soil piping is an important agent of erosion in many environments, including blanket peatlands. Peatland restoration that aims to reduce erosion has mainly focussed on revegetation and blocking ditches and gullies, rather than reducing erosion from natural soil pipes. However, little is known about the contribution of pipeflow to the fluvial carbon budget of degraded blanket peatlands and whether it is possible to moderate it. In a heavily degraded blanket bog, dissolved and particulate organic carbon (DOC and POC), and water colour, from two catchments were compared before and after half of the pipe outlets in one catchment were blocked. One blocked pipe was monitored for discharge and water quality both pre- and post-blocking as new pipe outlets had formed around the blocked outlet. Both pre- and post-blocking, maximum concentrations of DOC and POC were markedly higher in pipe-water than stream-water, with ratios of 1.2 (pre) and 1.3 (post) for DOC, and 4.8 (pre) and 8.8 (post) for POC, rendering pipe-to-stream transfer more effective for DOC than POC due to the deposition of POC close to pipe outlets. The increase in DOC and POC flux post-blocking in both catchments was near-identical, suggesting pipe outlet blocking was ineffective in reducing fluvial carbon export from pipe networks. Extrapolation of pipe fluxes to catchment scale showed pipes potentially contribute ~56 % of DOC exported by the stream, and that more POC was produced by pipes than was exported by the stream. Our work highlights that pipes need to be considered when seeking to reduce fluvial carbon export in degraded blanket peatlands.

1. Introduction

Peatland ecosystems are an important store of terrestrial carbon globally (Leifeld and Menichetti, 2018). However, degradation of peatlands is of major concern for releasing that stored carbon to the atmosphere and hydrosphere. While most peatland types occur on very gentle gradient landscapes, blanket peatlands are particularly susceptible to erosion due to their sloping nature (up to 15°). These peatlands have been projected to be at high risk from erosion in the northern hemisphere under future climate change (Li et al., 2017). The British Isles host around 10 % of global blanket peatland, but a substantial proportion is severely degraded as a result of peat abstraction, drainage, overgrazing, burning, and atmospheric pollution (Evans and Warburton, 2007; Smart et al., 2010; Ward et al., 2007). In particular, the southern Pennines of England carry the scars of a legacy of atmospheric deposition of metals (Rothwell et al., 2005), acidifying pollutants, and overgrazing which has resulted in highly degraded systems, where gully development has occurred as a result of damage to surface vegetation (Bower, 1961; Evans and Warburton, 2007; Yeloff et al., 2006). The extent and severity of this peatland erosion indicates the rapid destabilisation of the carbon store, with the peatland acting as a net exporter of carbon rather than a sink (Evans et al., 2006b). The erosion of these systems has led to rapid reservoir sedimentation downstream (Labadz et al., 1991).

Recent research into blanket peatland degradation has examined landform structure (Chico et al., 2020), hydrological function (Holden et al., 2011), processes controlling gully erosion (Evans and Lindsay, 2010), the production, loss and fate of particulate organic carbon (POC) and dissolved organic carbon (DOC) in runoff (Li et al., 2019; Palmer et al., 2016; Pawson et al., 2012), and metal and nutrient pollution of watercourses (Gaffney et al., 2021; Rothwell et al., 2005). Recent work has also examined the impacts of restoration action such as exclusion of grazing (Valdeolivas et al., 2018), re-vegetation (González and Rochefort, 2018), ditch blocking, gully blocking and re-vegetation on runoff production (Shuttleworth et al., 2019), and DOC and POC concentrations and fluxes in stream water (Evans et al., 2016; Peacock et al., 2018; Renou-Wilson et al., 2019; Shuttleworth et al., 2015). However, pipe erosion has been found to be prevalent in blanket peatlands (Holden, 2005a; Jones et al., 1997) and yet has received much less attention in terms of DOC and POC production in degraded systems and there is a lack of knowledge of whether peatland restoration action should target pipes.

Research into reducing erosion from soil piping is an overlooked issue in soil erosion control (Bernatek-Jakiel and Poesen, 2018). Piping is widely considered an important agent of subsoil erosion in both natural and modified landscapes (Bernatek-Jakiel and Poesen, 2018), especially where pipe roof collapse aids gully formation (Marzolff and Ries, 2011; Wilson, 2011; Xu et al., 2020). Soil pipes provide a fast route for throughflow and facilitate transport of large quantities of water, eroding soil from the inside out whilst entraining solutes and nutrients along the way (Anderson et al., 2009; Anderson and

Burt, 1982; Baillie, 1975; Faulkner, 2013; Rapson et al., 2006; Sayer et al., 2006; Verachtert et al., 2011). In blanket peatlands, where pipe density has been enhanced by management such as ditch drainage or burning of shrub cover for gun sports (Holden, 2005b), there is concern about greater rates of sediment and carbon loss from the peatland system which may have negative impacts on downstream ecosystems (Brown et al., 2019). While some data exist on the concentration and fluxes of DOC and POC in peatland pipe-water, it is predominantly from more intact peatland systems in the northern Pennines of England (Holden et al., 2012) or organo-mineral soils in Wales (Chapman et al., 1993), rather than highly eroded peatlands.

In some regions, peatlands are a major source of drinking water (Xu et al., 2018). A key issue for water companies over the last ~30-40 years in northern Europe has been the rising trend in water colour (Chapman et al., 2010; Hongve et al., 2004; Watts et al., 2001; Worrall et al., 2003) as a result of increasing DOC concentrations in streams draining organic soils (de Wit et al., 2016; Evans et al., 2006a). Deterioration in water colour complicates water purification for water companies (Bonn et al., 2010; Fearing et al., 2004; Van der Wal et al., 2011) and also has health implications as the chlorination of highly coloured water can result in the production of carcinogenic disinfection-by-products such as trihalomethanes (Valdivia-Garcia et al., 2016). In addition, the potential environmental implications of the increasing trend in DOC are wide ranging, from local effects on water transparency (Williamson et al., 2015), acidity (Urban et al., 1989), and metal toxicity (Rothwell et al., 2007; Tipping et al., 2003) through to effects on aquatic flora and fauna (Ramchunder et al., 2012). Therefore, reducing DOC production and subsequent export is an important motivation for peatland restoration. However, blanket peatland restoration techniques have typically targeted ditches and gullies (Parry et al., 2014), rather than pipe networks. While previous work has shown that in intact peatland systems pipes contribute significantly to POC and DOC fluxes at the catchment scale (Holden et al., 2012), to date, there has been little research on how blocking pipe outlets affects DOC and POC concentrations and fluxes in pipe- and / or stream-water, especially for highly eroded/degraded peatlands.

One approach to tackling piping in degrading peatland systems is to attempt to reduce sediment flux by blocking pipe outlets. To date, the impacts of pipe outlet blocking have only been studied in the context of its effects on stream and pipe hydrology (Regensburg et al., 2021). It remains unclear if pipes in more degraded blanket peatlands such as those found in the southern Pennines of England yield larger fluxes of aquatic carbon than observed in more intact blanket bog. Nevertheless, local peatland practitioners are keen to develop a better understanding about whether blocking pipe outlets provides wider benefits for preservation of ecosystem services through erosion control, including reduced discoloration of stream-water and sedimentation of downstream reservoirs. There is a need for further research to inform peatland practitioners as to whether pipe blocking should be included in future restoration initiatives in order to meet carbon export reduction objectives.

Here we report on an experiment investigating the impact of pipe outlet blocking on the concentrations and fluxes of DOC and POC in stream- and pipe-water in a heavily degraded blanket bog. Using a 'before-after-control-impact' approach with paired catchments and routine sampling before and after pipe blocking this paper aims to:

1) Determine how pipe concentrations and flux of POC and DOC compare to fluvial carbon output in streams;
2) Investigate whether pipe blocking results in a decrease in POC and DOC concentration and flux in stream-water.

2. Materials and methods

2.1. Study site

For this study, two sub-catchments were monitored in Upper North Grain (UNG), which is a small headwater (49 ha, Figure 1) on the edge of the Bleaklow Plateau in the South Pennines of the UK, draining into the River Ashop. The River Ashop provides a major inflow to Ladybower Reservoir, which forms an important source of potable water in the region. UNG experiences a maritime temperate humid climate with a mean annual rainfall of 1313 mm (2006 - 2013) which is evenly distributed over the year and a mean annual temperature of 6.9 °C (Clay and Evans, 2017). Altitude ranges from 531 to 467 m above sea level at the catchment outlet. The topography is characterised by steep slopes up to 15 ^{o} closer to the peat margin in the middle of the catchment, while most gullies occur on more gentle gradient hillslopes ranging from 0 to 7 ^{o}. The catchment is underlain by relatively soft shale grits with scattered exposed outcrops of the more resistant Millstone Grit (Wolverson Cope, 1998). The grits are overlain with a continuous cover of blanket peat of the Winter Hill Association (Jarvis et al., 1984). Dissection of the blanket peat in UNG is characterised by shallow branching gullies and peat hags on the flat summits (Bower Type I), whereas the sloped terrain in the catchment is incised by a network of active, mostly unbranched gullies (Bower Type II) (Bower, 1961), exposing the underlying geology in the lower sections. The UNG catchment is dominated by a heather, bilberry and cotton grass vegetation assemblage, which is lightly grazed by sheep (Rothwell, 2006). The two sub-catchments included in this study run north-to-south (Figure 1), and include gullies with incision up to 4 m deep into the peat. The extensive dissection by gully erosion and consequent exposure of bare peat on gully walls means that rates of POC production by surface erosion are high. Measured POC fluxes from UNG vary from 74.0 to 95.7 g C m^{-2} yr^{-1} (Evans et al., 2006a; Pawson et al., 2008), and are on the high end of values measured across the South Pennine region (3.4 - 90 g C m^{-2} yr^{-1}) (Billett et al., 2010), with strong connectivity of bare peat surfaces to the stream drainage network (Evans et al., 2006b). Details about the onset of peat erosion and gullying at UNG were described by Regensburg et al. (2020).

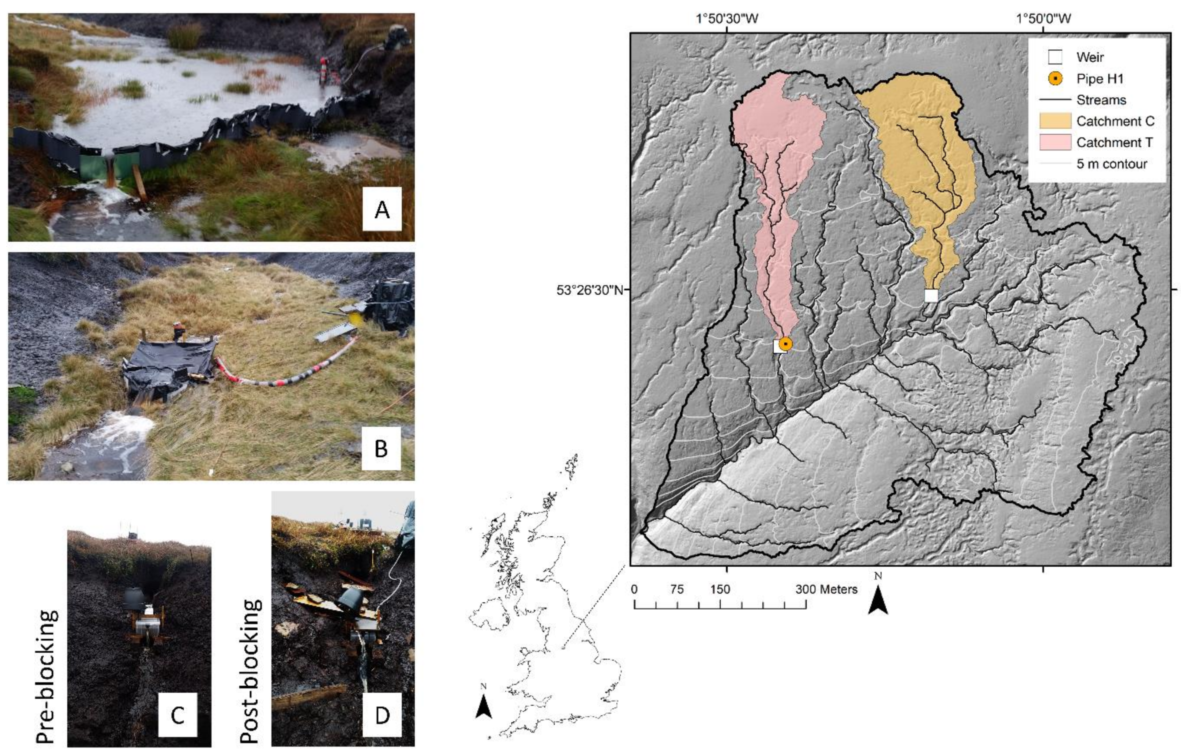

Figure 1. Left panel: A) outlet of catchment C, B) outlet of catchment T, C) outlet of pipe H1 pre-blocking, and D) outlet of pipe H1 post-blocking. Right panel: map of UK showing location of UNG, with inset of the monitored sub-catchments superimposed on a hillshade of the catchment, showing locations of each catchment weir (white rectangle) and pipeflow gauge at outlet of pipe H1 (orange circle).

2.2. Experimental design

To investigate the impact of pipe outlet blocking on fluvial carbon export, fluxes of POC and DOC from two streams were compared. Pipe outlet blocking treatments were installed in the catchment of one stream, hereafter called ‘catchment T’. The pipes in the catchment of the other stream were left untouched and the catchment functioned as a control, hereafter called ‘catchment C’. Suitable locations for weir placement were identified by walking upslope in the respective gully network, taking into account the possibility to perform salt dilution gauging immediately up or downstream of the weir. The area upslope of the weirs was estimated using a Digital Elevation Model obtained from LiDAR (MFFP, 2014), resulting in an estimated surface catchment of 4.32 ha for catchment C and 3.75 ha for catchment T.

Pipe surveys at UNG as reported by Regensburg et al. (2020) showed that the largest pipe outlets were usually found in gully sections with signs of headward retreat (referred to as head pipes: ‘H’) as opposed to smaller pipe outlets along the edge of straight gully sections (referred to as edge pipes: ‘E’). Considering the large diameter of head pipes, it was assumed such pipes would actively contribute to gully formation, and therefore, outflow from one head pipe in catchment T, hereafter referred to as pipe H1, was sampled to investigate the relative fluvial carbon contribution of pipe-water to stream-water. Based on 107 storm hydrographs, Regensburg et al. (2021) characterised pipe H1 as ephemeral. Between August and September 2019, 68% of the pipe outlets in catchment T were blocked. This represented a total of 31 pipe outlets, which were blocked with either a plug-like structure (n = 6) or a vertical screen (n = 25, including pipe H1) (for details see Regensburg et al. (2021)). On 27 September 2019, a further 20 pipe outlets were identified in two tributaries of catchment T. These tributaries had stone and wooden dams in them as part of earlier restoration activity (Regensburg, 2020), but none of their pipe outlets were blocked. In this paper the results focus on the combined impact of pipe outlet blocking methods on POC and DOC loss from catchment T. Monitoring of the streams and pipe H1 ran from 1 December 2018 to 29 February 2020, but the data for analyses was divided into two periods: a pre-blocking period (1.12.18 – 31.08.19) and a post-blocking period (1.09.19-29.02.20).

2.2.1. Discharge monitoring

Rainfall data were collected at three locations within each sub-catchment using an automated tipping bucket gauge (DAVIS AeroCone) with 0.2 mm resolution and a bulk rain collector at each location. For the period between December 2018 and February 2020, at least three of the six rainfall gauges across UNG were active at the same time. Therefore precipitation levels were derived by averaging recorded data across any of the active rainfall stations at an interval resolution of 5 minutes (for details see Regensburg et al. (2021) - Appendix B). Stream discharge was gauged at the outlet of each catchment by insertion of a weir plate using a calibrated V-notch. The water level above the notch was recorded using a vented pressure transducer (In-Situ Troll 500) that was placed in a stilling pool ~1 metre upstream of the weir plate. Stage was recorded at 5-minute intervals. When discharge was < 0.5 litre per second, a stage discharge relationship was determined by measuring the volume of water per unit of time using a measuring cylinder and stopwatch. At faster flows, discharge was estimated using salt dilution gauging in a 10 m straight section immediately downstream of the weir plate. Streamflow monitoring commenced in October 2018 for catchment T and in December 2018 for catchment C.

2.2.2. Water sampling

Pipe water from the outlet of H1 was channelled via guttering into a rectangular plastic box of 140 mm x 340 mm x 220 mm with a 22.5^{o} V-shaped opening, hereafter referred to as the "pipeflow gauge", which was instrumented with a vented pressure transducer (In-Situ Troll 500). Pressure readings above the sensor head in the box were recorded at a 5-minute interval. Gutters from the pipe outlet to the pipeflow gauge were shielded from rainfall using waterproof tape, polyethylene plastic sheeting, or wooden planks. During field visits, when water was flowing over the notch of the V, discharge from the pipeflow gauge was measured using a measuring cylinder and a stopwatch. A stage-discharge relationship for pipe H1 was derived by aggregating data from the calibration measurements on four pipeflow gauges in UNG (H1, H2, E1, and E2) (Regensburg et al., 2021). For this study, discharge monitoring at pipe H1 covered the period between May 2018 and February 2020. After blocking the outlet of pipe H1, any water that appeared from newly formed outlets and the blocked outlet was redirected to its respective pipeflow gauge using guttering to quantify the amount of water escaping from the blocked pipe. Water sampling

Water sampling started in December 2018, and covered a pre-blocking period of 8.5 months ("pre"), and a post-blocking period of 6 months (September 2019 – February 2020) ("post"). ISCO 3700 portable automatic water samplers (Teledyne Isco, Inc., Lincoln, NE, USA) were installed in the stilling pools located at straight stream sections of catchment C and catchment T, at least 1 m upstream of their respective weirs. The inlet for an ISCO 6712 portable automatic water sampler (Teledyne Isco, Inc., Lincoln, NE, USA) was installed in the pipeflow gauge at the outlet of pipe H1. Samples of pipe- and stream-water (500 mL) were collected using two different temporal resolutions: 1) storm events triggered the samplers to collect 24 water samples of 0.5 L at irregular intervals of maximum 30 minutes, or 2) at regular intervals of either 6 or 12 hours for a period of up to twelve consecutive days, with sampling being started manually during field visits. Storm sampling sequences were activated on nine occasions during the pre-blocking period until the end of May 2019, though not all automatic samplers were trigger simultaneously. Thereafter water samples were collected at regular set intervals. Water samples were collected from the field site on a fortnightly basis and stored in a dark, cold room at 4 °C before analysis to minimise decomposition of the aquatic carbon.

2.3. Water sample analyses

POC was estimated by loss-on-ignition of the residue from 500 mL water samples. Samples were filtered through pre-ashed (550 °C, 5.5 h), pre-weighed 0.7 mm Whatman GF/F glass micro-fibre filters using suction filtration equipment. The filtrate was dried at 105 °C for 24 h, weighed, and then ignited at 375 °C for 16 h in a muffle furnace and re-weighed (Dawson et al., 2002) to determine the suspended sediment in mg L^{-1}. All samples were weighed in grams with a five decimal place calibrated balance (Sartorius MSE125P-000-DU). The POC content of the suspended sediment was then calculated using a regression equation for non-calcareous soils (Ball, 1964).

Water colour was determined on all samples while DOC was determined on approximately one third of the total collected samples. Water colour and concentration of DOC were determined on 10-15 mL subsamples that were filtered through pre-washed 0.45 µm nylon syringe filters (Avonchem SF-3020) and stored in centrifuge tubes (Sarstedt) at 4 °C until analysed. Prior to analysis of DOC, the subsamples were acidified and sparged with oxygen in order to stabilise the sample and to remove any inorganic carbon. DOC in water was then determined using a Multi N/C 2100 combustion analyser (Analytik Jena), which has a detection limit of 50 µg L^{-1} with the DOC concentration determined by a calibration curve created using the standard DOC calibration compound, potassium hydrogen phthalate (KHP) and standard DIC stock solution. Regular analysis of KHP standards and use of a certified reference material, VKI QC WW4A, were used to check instrument performance during each run of samples. Water colour was measured using a UV-VIS spectrophotometer (Jasco V-630), using deionised water as a blank control. Absorbances were recorded in quartz cuvettes at wavelengths of 254, 400, 465 and 665 nm and reported in au m^{-1}. For each sample the E2:E4 (absorbance at 254 nm/absorbance at 400 nm), E4:E6 (absorbance at 400 nm/absorbance at 665 nm) and E2:E6 (absorbance at 254 nm/absorbance at 665 nm) ratios were calculated to characterise the seasonality of the coloured portion of dissolved organic matter. Where samples were analysed in duplicate or triplicate the mean value was determined and used in all further data analyses.

2.4. Data processing

All water samples collected when the instantaneous discharge at the stream or pipeflow gauge was zero were omitted from data analyses. POC samples were then checked for inconsistencies in the weighing procedure using a four point quality control (see for details Supplementary Information Appendix A). Concentrations of DOC which were determined initially as described above, are referred to as cDOC. The Specific Ultraviolet Absorbance (SUVA) for water samples was determined by dividing absorbance at 254 nm by cDOC. Absorbances at wavelengths 254 nm and 400 nm were both tested as a predictor of DOC concentration using linear relationships. For catchment C, catchment T, and pipe H1, absorbance at 254 nm provided the best predictor of DOC concentration with R squared values of 0.97, 0.95 and 0.97, respectively. Conversion functions for absorbance at 254 nm and 400 nm to DOC concentration are provided in Table S1. Hereafter, the derived relationships for DOC using absorbance at 254 nm, referred to as DOC_{254}, were used to characterise the distribution of concentration and flux of DOC for each outlet. Daily mean fluxes of POC and DOC_{254} from pipe H1 and catchments C and T were calculated using the following equation (Walling and Webb, 1985):

$$Flux = \frac{K \cdot \sum_{i=1}^{n}(Q_i \cdot C_i)}{\sum_{i=1}^{n} Q_i} \cdot Q_r \qquad \text{eq. 1}$$

where *K* is a conversion factor to scale measurement intervals to an hourly frequency, $Qi*C_i$ as the product of concentration *Ci* measured at an instantaneous discharge *Qi* forming the instantaneous flux in mg s^{-1}, and Q_r as the hourly mean discharge. Instantaneous discharge and instantaneous flux are both summed over n samples that were available for each hour, which may have varied during the monitoring period. Flux was expressed as an hourly mean export weight of dissolved or particulate organic carbon in kilograms. Then for each outlet the calculated hourly DOC and POC flux was plotted over the hourly mean discharge to derive a linear function of the form y = a x + b. All functions were forced through the origin for simplification. The relationships are depicted in Table 1. For each outlet, the functions were used to convert available discharge data to flux, which were then summed to obtain a total yield per outlet, for each season respectively.

Table 1. Overview of calibration functions for DOC and POC flux. The quality of line fit for slope a is indicated by the r squared value for each outlet and flux variable respectively.

	Flux as function of hourly discharge, *Qr*					
	Hourly DOC flux			Hourly POC flux		
	a	r^2	n samples	a	r^2	n samples
Catchment C	0.0667	0.7455	130	0.0497	0.4298	233
Catchment T	0.0611	0.8464	176	0.0172	0.4776	200
Pipe H1	0.0638	0.7827	116	0.0502	0.3092	86

To compare fluxes between pipes and streams, discharge for each outlet was standardised by calculating the exceedance probability for each outlet respectively between 1 December 2018 and 29 February 2020, using the following formula:

$$P_{exceed} = \frac{average\ rank}{n+1} \qquad \text{eq. 2}$$

with P_{exceed} expressing the percentage chance that a set discharge may be equalled or exceeded, using the $average\ rank$ of a discharge for a list of n number of recorded discharge intervals. The average rank was chosen here to correctly detect the prevalence of equally-sized discharges, particularly in low flow conditions. To investigate how the influence of discharge on concentrations and fluxes of fluvial carbon varies across outlets, for each outlet the discharge was categorised to either above or below its respective median (Figure 2). An exceedance probability ≤ 50 % was categorised as above median discharge (“AMD”), and all else below median discharge (“BMD”). Flow duration curves for both catchments and pipe H1 are provided in Figure S1. Discharge continuity was determined for each outlet for the periods March-April-May (MAM), June-July-August (JJA), September-October-November (SON), and December-January-February (DJF).Datasets did not follow a normal distribution, even after transformation, and therefore non-parametric tests of association were employed. Due to varying water sampling intervals among all outlets, comparisons between sample pairs of variables or outlets were performed by association using Kendall's Tau (2-tailed, α = 0.01).

3. Results

3.1. Water budget

Rainfall was 886 mm and 931 mm for the pre-blocking period and post-blocking period respectively (Figure 2). Runoff was 26 and 54% higher in the post blocking period (857 mm versus 935 mm) than the pre blocking (678 mm versus 607 mm) for catchment C and T respectively. (Figure 2). Pipe H1 produced 452 m^3 of discharge in the pre-blocking period compared to 807 m^3 in the post-blocking period and contributed to 2.0 % and 2.3 % of stream discharge in catchment T in each intervention period, respectively (Table 2).

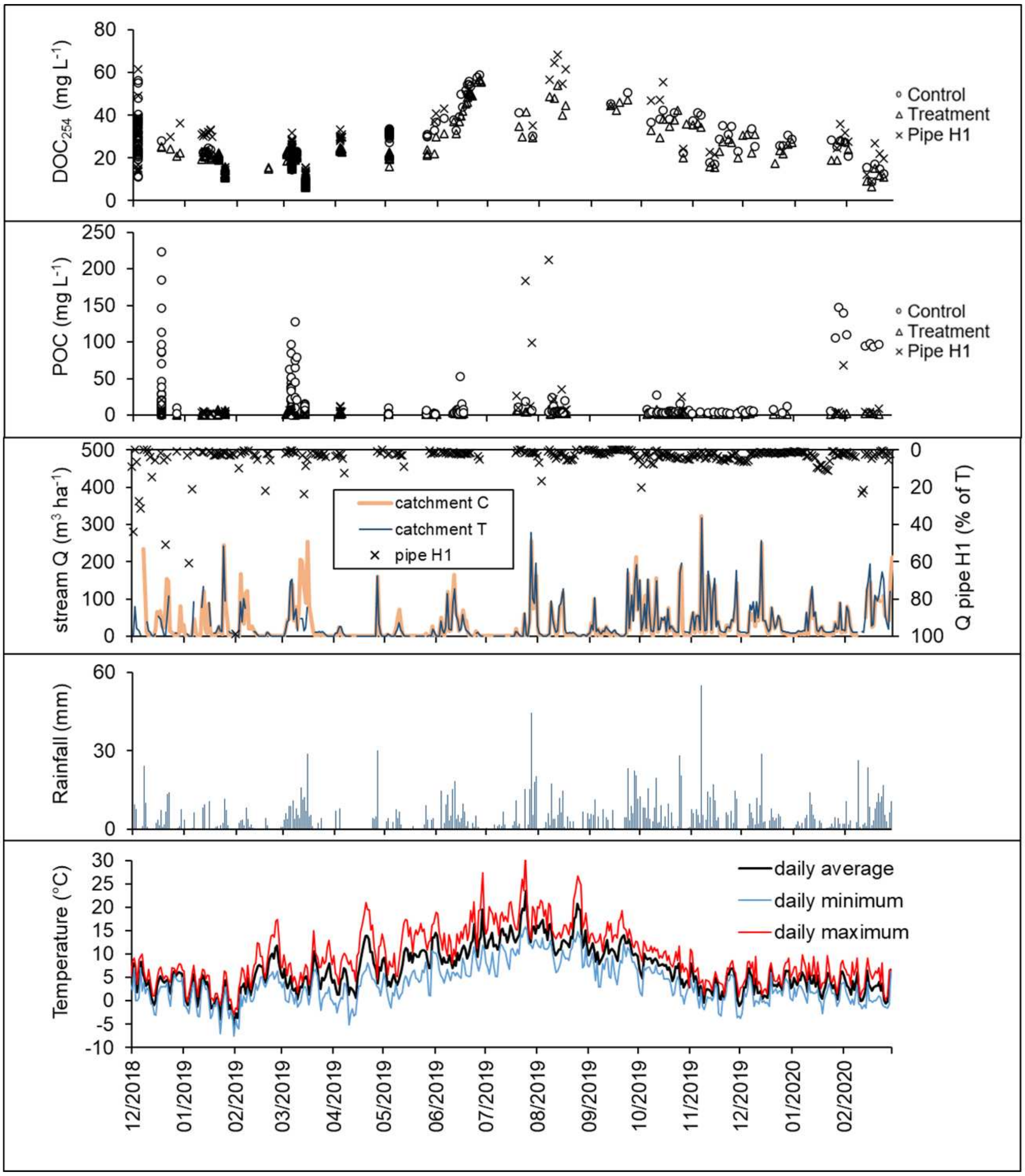

Figure 2. Timeseries plot of sampled concentrations of DOC_{254} and POC in mg L^{-1}, and daily totals of stream discharge (m^3 ha-1) and pipe discharge (% of catchment T), rainfall (mm) and temperature (°C), for each outlet (catchment C, catchment T, and pipe H1) over the whole monitoring period.

For all outlets, the duration for which flow over the weir was observed (AMD + BMD) was markedly longer in the post-blocking period with flow durations 1.91, 1.90, and 1.12 times longer for catchment C, catchment T, and pipe H1 respectively compared to the pre-blocking period (Table 2). In the pre and post-blocking period, the fraction of flow above and below median discharge was similar for both catchments (Table 2). Zero flow over the weir occured more often in catchment C than in catchment T during the whole monitoring period, with 37 % versus 23.4 % of the time respectively, with the largest difference (NF: C = 23 % vs T = 2.3 %) observed over September, October, November (SON)-2019 (Table 2). Periods with relative short flow duration in catchment C occurred in spring and summer; 35 % of the time in MAM-2019 and 38.4 % in JJA-2019 (Table 2). The period with the shortest flow duration for catchment T was observed in MAM-2019 with flow occurring 41.3 % of the time (Table 2).

Overall, pipeflow at the outlet of pipe H1 did not decrease after pipe outlet blocking, as pipeflow was produced 86.1 % of the time in the post-blocking period compared to 76.4 % in the pre-blocking period. The discharge distribution around the median was strongly skewed for pipe H1 in both intervention periods, with a smaller percentage of flow pre-blocking being above the median as opposed to below, while in the post-blocking period the opposite was observed because it was wetter (Table 2). Dividing the fraction of time pipe H1 produced discharge by that of catchment T showed that pipe H1 flowed more than catchment T in the pre-blocking period with pipe H1 being 1.58, 1.99 and 1.09 more active compared to catchment T in DJF-2018, MAM-2019, JJA-2019 respectively. In the post-blocking period, pipe H1 was less active than catchment T with ratios of 0.83 in SON-2019 and 0.95 in DJF-2019 (Table 2).

Table 2. Summary of hydrological responses for each outlet (C = catchment C, T = catchment T, P = pipe H1), for the pre- and post-blocking period in terms of discharge distribution over time, in % (NA = data error, NF = no flow, AMD = above median discharge, and BMD = below median discharge). Runoff Coefficient (RC) was calculated for streams in %, and for pipe H1 details on runoff are provided as the percentage that pipeflow from H1 contributed to streamflow in catchment T (% of T).

Period	Season	Outlet	Discharge distribution, % of time				Runoff	
			NA	NF	AMD	BMD	RC (%)	% of T
pre-blocking	DJF-2018 (P = 225 mm)	C	7.7	29.9	36.5	26	115.4	
		T	15.6	27.5	32	24.9	111.3	
		P	7.6	2.2	68.5	21.7	-	1.8
	MAM-2019 (P = 275 mm)	C	0	67.2	13.2	21.8	77.5	
		T	9.1	49.5	23	18.3	49.9	
		P	2	17.9	60.6	21.7	-	2.7
	JJA-2019 (P = 386 mm)	C	0	63.8	18	20.4	53.1	
		T	8.9	36.2	31.4	23.4	56.7	
		P	0	42.3	26.4	33.5	-	1.8
	total (P = 886 mm)	C	2.5	52.8	22.2	22.4	76.5	-
		T	11.2	37.8	28.8	22.2	68.5	-
		P	3.2	20.5	51.1	25.3	-	2
post-blocking	SON-2019 (P = 544 mm)	C	0	23	37.4	40.7	77.5	
		T	0.8	3.2	44.6	51.5	83.5	
		P	2.8	18.2	15.5	64.6	-	2.4
	DJF-2019 (P = 388 mm)	C	3.3	3.5	53.9	40.4	97.7	
		T	2	0	45.6	52.4	111.4	
		P	6	1.1	36.7	57.3	-	2.3
	total (P = 931 mm)	C	1.6	13.1	45.1	40.1	85.9	-
		T	1.4	1.6	45.1	52	95.2	-
		P	4.4	9.6	25.8	60.3	-	2.3

3.2. Concentrations of DOC and POC

Water colour, and hence DOC_{254} concentrations, in pipe- and stream-water displayed a clear seasonal cycle with highest concentrations observed in summer and lowest in winter, regardless of increasing discharge over the monitoring period (Figure 2). DOC_{254} was positively correlated to temperature for catchment C ($\tau = 0.219$, $p < 0.001$, $\alpha = 0.01$) and pipe H1 ($\tau = 0.157$, $p = 0.003$, $\alpha = 0.01$), with R squared values of 0.30 and 0.14 respectively, but no correlation for temperature and DOC_{254} was found for catchment T ($\tau = 0.077$, $p = 0.061$, $\alpha = 0.01$) (Figure S2). Over the entire monitoring period in both catchments, DOC_{254} concentrations ranged between 5-29 mg L^{-1} during the winter and 30-59 mg L^{-1} in the summer (Table S2), and DOC_{254} in pipe-water peaked at 68.5 mg L^{-1} in summer and 36 mg L^{-1} in winter (Table S2). Plotting DOC_{254} over discharge of the respective outlets showed a negative relation, which was particular visible for pipe H1 (Figure S3). In contrast, POC concentrations seemed much more episodic and no clear relationship with discharge was observed (Figure S3). DOC composition, measured as SUVA, did not vary much over the monitoring period (Figure 2). In the pre-blocking period, stream-water DOC_{254} concentration ranged from 6.2 to 58.9 mg L^{-1} and 6.7 to 50.8 mg L^{-1} in the post-blocking period. Pre-blocking and post-blocking, DOC_{254} concentrations were similar for both catchments, with a median value of 22.3 mg L^{-1} pre- and 28.8 mg L^{-1} post-blocking for catchment C, and a median DOC of 20.6 mg L^{-1} pre-blocking and 27.6 mg L^{-1} post-blocking for catchment T (Figure 3).

Pipe-water DOC_{254} concentrations were slightly lower post-blocking with a median concentration of 29.7 mg L^{-1} pre- and 27.1 mg L^{-1} post-blocking, whereas POC concentrations were slightly higher post-blocking with a median of 3.4 mg L^{-1} pre and 4.5 mg L^{-1} post-blocking (Figure 3). The maximum concentration of DOC_{254} for pipe H1 was similar for the pre- and post-blocking monitoring periods, with 68.5 mg L^{-1} pre and 61.7 mg L^{-1} post pipe outlet blocking. Despite pipeflow being observed more frequently in the post-blocking period, especially for above median discharge, the largest POC concentration of 212.2 mg L^{-1} was observed in the pre-blocking period for pipe H1 (Figure 3).

The median POC concentration was similar across intervention periods for each catchment, although median POC concentration for catchment C was about three times larger than that observed for catchment T. In the post-blocking period, the maximum POC concentration in catchment C was markedly larger than in the pre-blocking period (311.3 mg L^{-1} post-blocking compared to 127.5 mg L^{-1} pre-blocking), while the maximum POC concentration in catchment T was markedly lower in the post-blocking period, 7.7 mg L^{-1} compared to 44.6 mg L^{-1} in the pre-blocking period (Figure 3).

Pipe-water DOC_{254} concentrations ranged from 4.6 to 68.5 mg L^{-1} in the pre-blocking period, and 9.1 to 61.7 mg L^{-1} in the post-blocking period (Table 3). Pipe-water POC concentrations ranged from 0.3 to 212.2 mg L^{-1} in the pre-blocking period, and from 2.0 to 67.7 mg L^{-1} in the post-blocking period (Figure 3).

The maximum POC concentrations observed in catchment T were markedly lower than that observed in pipe H1, with concentrations up to 4.8 times lower in the pre-blocking period, and 8.8 times lower in the post-blocking period (Figure 3). The maximum DOC_{254} concentration of pipe H1 was greater than that of catchment T, but differences were smaller than observed for POC concentrations, with DOC_{254} concentrations of 68.5 versus 56.8 mg L^{-1} pre-blocking, and 61.7 versus 47.3 mg L^{-1} post-blocking, respectively (Figure 3). This suggests that the pipe-stream transfer of fluvial carbon is more effective for DOC than POC.

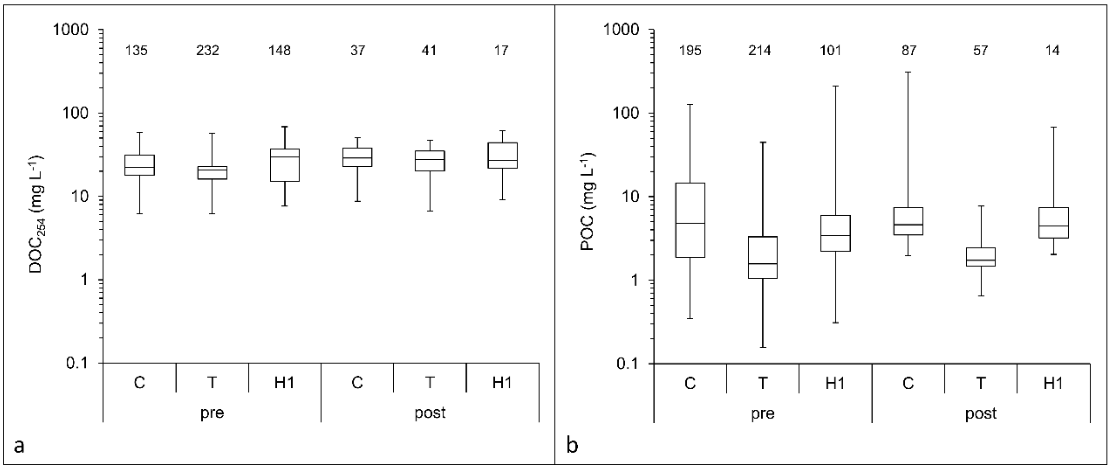

Figure 3. Boxplot of a) DOC_{254} (mg L^{-1}) and b) POC (mg L^{-1}) observed in streams (C = catchment C, T = catchment T), and pipe-water from pipe H1, for both intervention periods (pre- and post-blocking); for each outlet the number of included samples is listed above their respective boxplot. The whiskers indicate the minimum and maximum values.

3.3. Water colour

Table 3 shows that mean absorbances across the four measured wavelengths peaked in both pipe- and stream-water in summer and autumn, with mean absorbances up to three times higher than in other seasons. Ratios of E2:E4 and E4:E6 were similar for both catchments and pipe H1 over the whole monitoring period (Table 3), indicating that the composition of DOC was similar over the monitoring period, and most likely had the same source. In both winters of the study (DJF 2018 and 2019), E2:E6 was similar in pipe-water, but markedly higher compared to the ratios observed in catchment T and catchment C, most likely due to much higher absorbances at 254 nm in pipe-water compared to catchment T (Table 3).

Table 3. Summary of colour measurements for each outlet by season, showing mean absorbance at 254 nm, 400 nm, 465 nm, 665 nm, and mean Specific Ultraviolet Absorbance (SUVA). Ratios between absorbance at 254, 400 nm and 665 nm are included as E2:E4, E4:E6, and E2:E6 respectively.

	pre-blocking			post-blocking		
Catchment C	DJF-2018	MAM-2019	JJA-2019	SON-2019	DJF-2019	units
665.0 nm (n = 172)	1.1	0.8	2.4	1.9	1.0	AU m^{-1}
465.0 nm (n = 172)	6.8	5.6	15.9	12.4	7.0	AU m^{-1}
400.0 nm (n = 172)	15.9	13.1	36.2	27.3	16.0	AU m^{-1}
254.0 nm (n = 172)	104.1	89.4	223.2	163.3	101.2	AU m^{-1}
E2:E4	6.6	6.9	6.2	6.0	6.4	(-)
E4:E6	16.4	17.2	15.6	14.6	18.7	(-)
E2:E6	110.1	119.0	97.0	87.8	120.4	(-)
SUVA (n = 46)	ND	3.4	4.7	4.8	4.4	L mg^{-1} m^{-1}
Catchment T	DJF-2018	MAM-2019	JJA-2019	SON-2019	DJF-2019	units
665.0 nm (n = 273)	0.7	0.7	2.4	2.1	1.2	AU m^{-1}
465.0 nm (n = 273)	4.9	5.0	16.1	12.4	7.3	AU m^{-1}
400.0 nm (n = 273)	11.3	11.4	35.8	26.4	15.7	AU m^{-1}
254.0 nm (n = 273)	76.4	79.6	223.4	156.0	94.1	AU m^{-1}
E2:E4	6.9	7.1	6.3	5.9	6.2	(-)
E4:E6	17.3	16.8	14.8	12.8	18.1	(-)
E2:E6	119.7	120.3	93.2	75.5	118.3	(-)
SUVA (n = 88)	3.8	3.4	4.8	5.0	4.3	L mg^{-1} m^{-1}
Pipe H1 (n = 165)	djf-2018	mam-2019	jja-2019	son-2019	djf-2019	units
665.0 nm	0.9	1.0	6.7	2.5	1.0	AU m^{-1}
465.0 nm	7.6	7.9	23.3	15.3	7.4	AU m^{-1}
400.0 nm	17.5	17.9	46.4	33.0	16.4	AU m^{-1}
254.0 nm	120.4	119.5	267.8	197.2	104.3	AU m^{-1}
E2:E4	6.9	6.8	6.0	6.0	6.5	(-)
E4:E6	21.9	17.9	14.6	14.4	22.9	(-)
E2:E6	152.8	122.4	91.0	87.7	153.1	(-)
SUVA (n = 70)	3.8	4.2	5.1	4.6	4.5	L mg^{-1} m^{-1}

3.4. Fluxes of DOC and POC

Ranges of instantaneous flux varied across seasons for both catchments and pipe H1. For both catchments, concentrations of DOC_{254} peaked in summer, but their highest seasonal median instantaneous DOC flux was observed in spring (MAM-2019) (Table 4). In DJF-2018 the range of instantaneous DOC_{254} flux of catchment T was 2.34 times larger than that of catchment C, but in the wetter DJF-2019 the range of instantaneous DOC_{254} flux of catchment T was about a third smaller than that of catchment C (Table 4). The largest median instantaneous DOC flux for pipe H1 was observed in the autumn (SON-2019), after the pipe outlet was blocked (Table 4). The episodic nature of POC concentrations in both pipe- and stream-water (Figure 2), translated into a varied pattern in the instantaneous POC flux across seasons. This variation was particularly noted for catchment C, which showed large differences across seasonal medians, of up to two orders of magnitude (Table 4).

Table 4. Distribution of instantaneous flux of DOC_{254} and POC, as observed in streamflow (C = catchment C, T = catchment T) and pipeflow (P = pipe H1) over seasons.

season	outlet	Instantaneous DOC_{254} flux (mg s^{-1})				Instantaneous POC flux (mg s^{-1})			
		N	Median	Maximum	Range	N	Median	Maximum	Range
DJF-2018	C	19	28.1	154.0	152.9	37	8.8	780.6	780.5
	T	67	26.5	364.1	358.1	56	6.3	422.0	421.6
	P	52	1.0	7.0	7.0	35	0.5	2.3	2.3
MAM-2019	C	96	65.9	360.0	354.6	112	120.2	3265.6	3265.2
	T	137	42.1	283.8	283.4	110	9.0	2422.9	2422.8
	P	87	1.1	4.6	4.3	55	0.4	2.5	2.4
JJA-2019	C	20	45.2	731.4	726.2	46	23.5	1357.5	1356.9
	T	28	24.5	591.3	588.4	48	9.1	540.8	540.2
	P	9	1.5	8.9	8.8	11	1.8	46.9	46.8
SON-2019	C	21	50.4	334.9	332.8	72	9.3	1487.8	1487.7
	T	22	25.6	343.1	333.9	41	3.1	646.8	645.5
	P	8	2.8	21.1	20.1	6	0.6	51.0	50.7
DJF-2019	C	16	21.6	158.2	156.2	15	493.8	7181.1	7160.3
	T	19	19.8	113.5	105.2	16	5.9	204.7	203.0
	P	9	1.4	2.3	1.6	8	0.7	3.9	3.5

Across both monitoring periods, instantaneous DOC_{254} flux for both catchments responded in a similar way to discharge, while instantaneous POC flux in response to discharge differed markedly between them (Figure 4). The variation in the amplitude of instantaneous POC flux for the same discharge seems larger for catchment C compared to that of catchment T, in both monitoring periods. This effect was particularly noticeable in the post-blocking period, with maximum range of instantaneous POC flux over the same discharge spanning two orders of magnitude for catchment C compared to one order of magnitude for catchment T (Figure 4). In the pre-blocking period, instantaneous fluxes of DOC_{254} and POC in pipe H1 were roughly two orders of magnitude lower than that of catchment T. A similar trend was observed for pipe H1 in the post-blocking, but only for pipe discharges greater than the median (Figure 4).

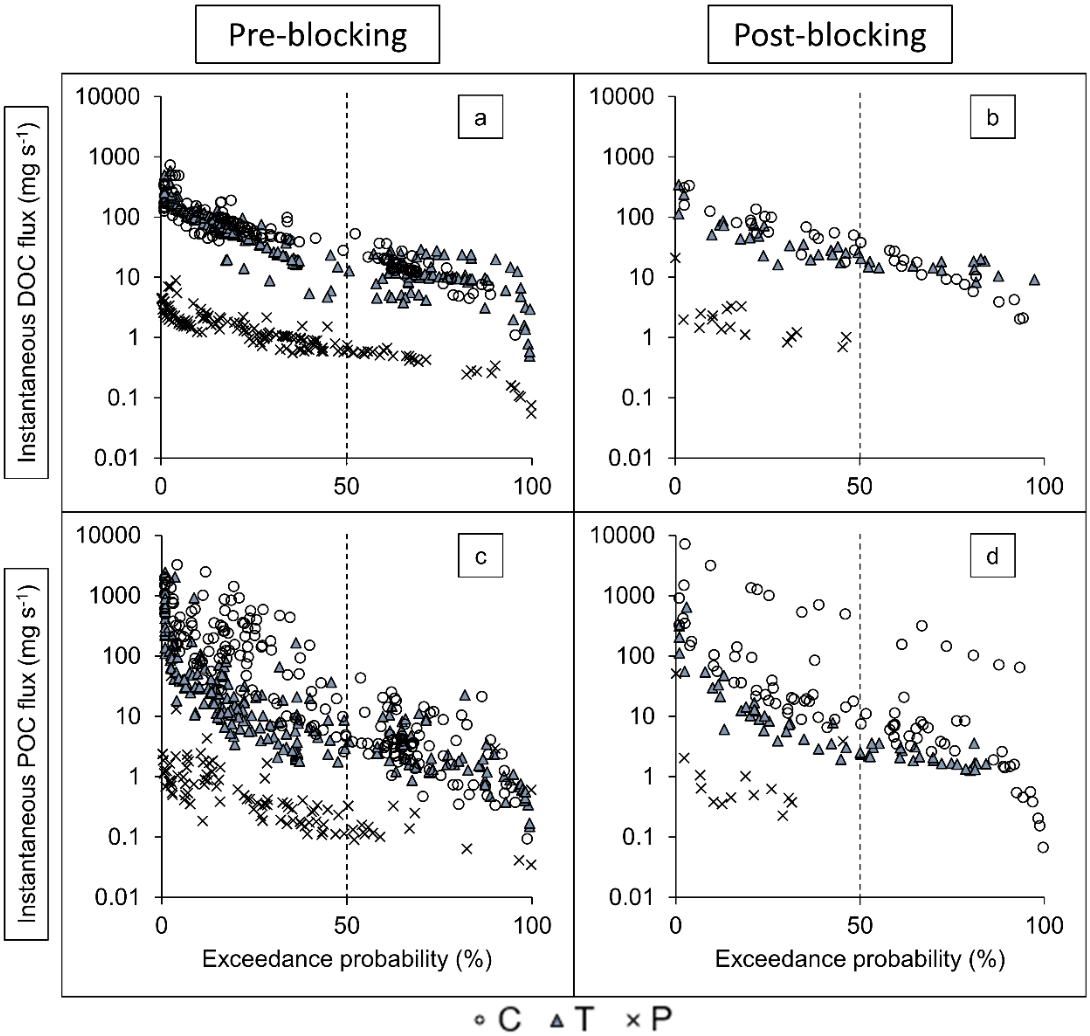

Figure 4. Scatterplots showing distribution of instantaneous flux for samples of DOC (mg s^{-1}) and POC (mg s^{-1}) over the exceedance probability of instantaneous discharge for each outlet (C = catchment C, T = catchment T; and P = pipe H1) across monitoring periods (pre- and post-blocking).

Table 5 provides a summary of the estimated yields of DOC_{254} and POC for each season, utilizing the relationships presented in Table 1. Catchment C yielded 525 kg DOC_{254} and 396 kg POC in the pre-blocking period, and 613 kg DOC_{254} and 462 kg POC in the post-blocking period (Table 5). Catchment T had a total estimated yield of 379 kg DOC_{254} and 107 kg POC in the pre-blocking period, and 555 kg DOC_{254} and 156 kg POC post-blocking (Table 6). Pipe H1 exported an estimated 8.0 kg DOC and 6.2 kg POC in the pre-blocking period, and 13.5 kg DOC_{254} and 10.5 kg POC in the post-blocking period (Table 5). The flux contribution to catchment T by pipe H1 was 2.11 % DOC_{254} and 5.8 % POC pre-blocking, and 2.43 % DOC_{254} and 6.73 % POC post-blocking.

In the pre-blocking period, above median discharges contributed to 96.2 % of the DOC_{254} flux and 93.2 % of the POC flux in catchment C , versus 87.2 % of the DOC_{254} flux and 87.2 % of POC flux in catchment T (Table 5). In the post-blocking period, a similar pattern was observed at the catchment outlet, showing above median discharge contributing 92.7 % of the DOC_{254} flux and 92.7 % of the POC flux in catchment C, and 89.0 % of the DOC_{254} flux and 88.9 % of the POC flux in catchment T (Table 5). Pipeflow above median discharge accounted for 72.5 % of the DOC_{254} flux and 71 % of the POC flux at pipe H1 in the pre-blocking period, and 93.3 % of the DOC_{254} flux and 94.3 % of the POC flux at pipe H1 in the post-blocking period (Table 5).

Table 5. Summary of total estimated flux of DOC (kg) and POC (kg) in streams (C and T) and pipe H1 (P), for seasons (DJF-2018, MAM-2019, JJA-2019, SON-2019, and DJF-2019) and flow types (BMD and AMD). For pipe H1, its contribution to catchment T is given as a percentage of the flux in catchment T.

		stream DOC flux		pipe DOC flux		stream POC flux		pipe POC flux	
		C (kg)	T (kg)	P (kg)	% of T	C (kg)	T (kg)	P (kg)	% of T
DJF-2018	AMD	183.2	137.3	2	1.4	137.9	38.6	1.5	4
	BMD	18.2	17.4	1	5.7	13.9	4.9	0.8	16.2
	Total	201.4	154.8	3	1.9	151.8	43.4	2.3	5.4
MAM-2019	AMD	157.1	72.9	1.6	2.1	118.4	20.5	1.2	6
	BMD	7.7	13.1	0.9	6.7	5.8	3.7	0.7	18.8
	Total	164.8	86	2.4	2.8	124.2	24.2	1.9	8
JJA-2019	AMD	149.4	120.5	2.2	1.8	112.5	33.9	1.7	5.1
	BMD	9.5	18.1	0.4	2	7.2	5.1	0.3	5.7
	Total	158.9	138.6	2.6	1.8	119.7	39	2	5.2
SON-2019	AMD	307.1	256.5	6.9	2.7	231.2	72.1	5.4	7.5
	BMD	19.3	29.6	0.3	1	14.8	8.4	0.2	2.7
	Total	326.4	286.1	7.2	2.5	246	80.5	5.6	7
DJF-2019	AMD	261.8	237.7	5.7	2.4	197.2	66.8	4.5	6.7
	BMD	25.2	31.5	0.5	1.7	19.1	8.9	0.4	4.8
	Total	287	269.2	6.3	2.3	216.2	75.7	4.9	6.5

4. Discussion

4.1. The effect of pipe outlet blocking on DOC and POC in pipe- and stream-water

Our study is the first, as far we are aware, to examine the influence of blocking natural soil pipes in blanket peat on downstream water quality. The control-treatment experimental design allowed us to examine whether impeding pipeflow through pipe outlet blocking had an impact on fluvial carbon export and water colour, at the stream and ephemeral pipe network scale.

Dividing median DOC and POC concentrations for the post-blocking period by the pre-blocking median concentration (as provided in Figure 3) results in ratios of 1.29, 1.34, and 0.91 for DOC_{254} and 0.96, 1.06, and 1.32 for POC, for catchment C, catchment T, and pipe H1 respectively. The similarity in the ratio for catchments C and T shows that blocking 48 % of the pipe outlets in catchment T had no impact on stream-water DOC and POC. While the median DOC_{254} concentration for pipe H1 was smaller post-blocking, its median POC concentration was markedly larger post-blocking, but both trends may have been skewed by a reduced sample size post-blocking. For both DOC_{254} and POC, regardless of a reduced sample size post-blocking, catchment T showed a stronger positive change in median concentrations than catchment C. In addition, throughout the monitoring period no change was observed in the composition of water colour for both pipe- and stream-water. Together, these findings suggest that pipe outlet blocking had no impact on pipe- and stream-water DOC and POC concentrations and is therefore not an effective method for reducing POC, DOC or water colour in degraded blanket peatlands.

We also showed that the pipe-to-stream flux of fluvial carbon was stable across the monitoring period, with increases of pipe flux for DOC_{254} and POC during a wetter post-blocking period. At the catchment scale, increases in DOC_{254} and POC flux post-blocking, as result of a wetter post-blocking period, were near identical for both catchments with ratios of 1.17 for DOC_{254} and 1.46 for POC, rendering the effect of pipe outlet blocking on fluvial C flux at the catchment scale marginal. Across the whole monitoring period, the variation in the seasonal POC flux was smaller for catchment T compared to that observed in catchment C. This difference may be caused by the presence of gully dams in the upper sections of catchment T into which a third of the identified pipes in catchment T drain. However, pipe blocking occurred downstream of these gully dams and, as such, our results did not indicate that pipe blocking had an effect on fluvial carbon fluxes in catchment T.

4.2. Fluvial carbon patterns at the catchment scale

DOC_{254} concentrations and stream-water absorbance levels for catchments C and T show a clear seasonal pattern, with elevated values observed between June and March, which is in line with multi-annual DOC and water colour records in peat-dominated catchments showing a strong temperature-dependency (Chapman et al., 2010). Observed summer and winter concentrations of stream DOC_{254} for catchments C and T (summer: 29.6 – 58.9 mg L^{-1}; winter: 6.7 – 33.5 mg L^{-1}), are consistent with those reported in previous studies on the wider eroded area of Bleaklow Plateau (Billett et al., 2010), but up to twofold higher than those observed in streams draining more intact peat of the northern Pennines in the UK, with 17 – 35 mg L^{-1} in summer and 7 – 15 mg L^{-1} in winter for Cottage Hill Sike (20 ha), and 7 – 23 mg L^{-1} in summer and 4 – 10 mg L^{-1} in winter for the larger catchment of Trout Beck (1150 ha) (Clark et al., 2007).

As pipe outlet blocking had no measurable effect on fluvial carbon concentrations in both pipe H1 and catchment T, we estimated the annual total DOC and POC flux for the catchments and pipe H1 in the calendar year 2019, MAM-2019 to DJF-2019 using equation 1. This enabled comparisons for overall erosion rates at catchment level (Table 6) and pipe-to-stream carbon transfers to be compared with those found in other studies (Table S3). Table 6 shows that the DOC flux for both catchments (catchment C = 21.7 g C m^{-2} yr^{-1}; catchment T = 20.8 g C m^{-2} yr^{-1}) is consistent with the DOC flux obtained at the catchment outlet of UNG (18.5 g C m^{-2} yr^{-1}) (Pawson et al., 2008) and similar in magnitude to DOC fluxes found in other vegetated blanket peat catchments in the region (Billett et al., 2010), northern Pennines of England (Holden et al., 2012; Worrall et al., 2009), Scotland (Dinsmore et al., 2010), and Wales (Billett et al., 2010). Fluxes of POC in the two sub-catchments of UNG were 5.9 – 16.4 g C m^{-2} yr^{-1} lower than the flux of 74 g C m^{-2} yr^{-1} reported at the catchment outlet by Pawson et al. (2008), indicating that, although pipes may contribute markedly to their POC budget, other additional POC sources exist in UNG. POC flux for the two sub-catchments was an order of magnitude smaller than that of smaller catchments with proportionally more bare surfaces (Li et al., 2019), but of similar magnitude to larger blanket peatland catchments in the UK (Dinsmore et al., 2010; Worrall et al., 2009). However, in this study samples were collected primarily at set time intervals, with additional water samples collected during some storms. Frequency of stream-water sampling is an important determinant for flux calculations (Pawson et al., 2008). For instance, the larger DOC and POC flux estimated for the stream at Cottage Hill Sike, as reported by Holden et al. (2012), may have resulted from a more intense sampling campaign, including water sampling during storms. The authors observed, when fluxes were based only on two-weekly sampling, much lower fluxes for DOC in the range of 29.7 - 36.5 g C m^{-2} yr^{-1}, which are consistent with those found for catchment C and T in UNG in this study. Information about piping frequency for catchments with DOC and POC flux data would aid interpretation of the role of piping in influencing peatland aquatic carbon fluxes.

4.3. Fluvial carbon patterns in pipe-water

Water colour in pipe H1 followed a similar temporal pattern to that of catchment T, but seasonal means of absorbance were higher than those observed in catchment T. As the composition of DOC was the same for pipe- and stream-water, water colour and DOC concentrations in pipe-water should be assumed to be temperature-dependent given the significant relationships observed. However, wider comparisons of specific controls on water colour from pipe-water do not exist, and need further research. In earlier work at UNG, POC concentration in stream-water was found to be positively related to discharge (Pawson et al., 2008), but for catchment C and T, and pipe H1, no such relationship was found (Figure S3).

To date, the only other comprehensive assessment of DOC and POC in pipe-water was conducted by Holden et al. (2012), investigating pipe-to-stream fluvial carbon transfer at Cottage Hill Sike, a relatively uneroded blanket bog in the northern Pennines of England. For the pre-blocking period, we observed a mean DOC concentration of 27.9 mg L^{-1} for pipe H1, which is very similar to that reported by Holden et al. (2012) for ephemeral and perennial pipes at Cottage Hill Sike (30.5 and 27.9 mg L^{-1}, respectively). Despite degrading blanket bogs being often associated with increased POC fluxes (Evans et al., 2006b), pipe-to-stream fluvial carbon transfer in UNG was more effective for DOC than POC concentrations, both pre- and post-blocking. However, pre-blocking, the mean POC concentration of pipe H1 (9.8 mg L^{-1}) was nearly twice that of ephemeral pipes and fourfold higher than that of perennial pipes at Cottage Hill Sike (5.4 and 2.2 mg L^{-1}, respectively) (Holden et al., 2012).

For calendar year 2019, we estimated that pipe H1 produced 18.5 kg DOC_{254} and 14.4 kg POC, which accounted for 2.37 % and 6.56 % of the DOC_{254} and POC flux, respectively, of catchment T (Table S3). The annual DOC_{254} flux in kg from pipe H1 was consistent with the average pipe DOC flux of 22.05 kg observed at Cottage Hill Sike, and the POC flux in kg from pipe H1 was similar to the flux observed from an ephemeral pipe (P8 – outlet 10 cm diameter) monitored at Cottage Hill Sike by Holden et al. (2012), which was ten times higher than any other ephemeral pipe monitored at Cottage Hill Sike . To compare pipe H1 to individual monitored pipes at Cottage Hill Sike, the area-weighted fluvial carbon flux for pipe H1 was calculated by dividing the sum of DOC_{254} and POC flux over 2019 by its maximum dynamic contribution area of 1152 m^2 (Regensburg et al., 2021), resulting in ~28 g C m^{-2} yr^{-1}. This area-weighted carbon flux is similar to that of large ephemeral and perennial pipes at Cottage Hill Sike (Holden et al., 2012), but pipe H1 alone has a larger area-weighed fluvial flux than catchment T (Table S3), which is in contrast to combined observations of pipes at Cottage Hill Sike (P1-8 < 26 g C m^{-2} yr^{-1} versus 57 g C m^{-2} yr^{-1} for the catchment outlet) (Holden et al., 2012). As POC flux from pipe H1 accounted for ~40 % of its total suspended sediment load, the area-weighted fluvial flux estimated for pipe H1 translates to ~70 t km^{-2} of particulate organic carbon, which alone is about 20 to 30 % of the organic sediment yield range estimated for the whole UNG catchment by Evans et al. (2006b). Such high rates support the speculative association between the onset of gullying and pipe development, a theory developed following the characterization of dominant erosion processes on degrading blanket bog by Bower (1961). However, beyond our work there is virtually no available evidence to test this widely discussed hypothesis, illustrating the need for further research on the link between pipe erosion and gully development in blanket peatlands.

Table 6. Summary of literature on DOC and POC fluxes in UK blanket peat catchments for which data was collected by periodic stream-water sampling.

catchment name	location	catchment area (km^2)	altitude (m amsl)	slopes (degrees)	mean annual precipitation (mm)	mean annual temperature (C)	DOC flux (g C m^{-2} yr^{-1})	POC flux (g C m^{-2} yr^{-1})	Notes	Source
Catchment T, Upper North Grain, S. Pennines*	53°26′28″N , 001°50′30″W	0.038			1592		20.8	5.9	blanket bog, severe erosion, 2019, DOC: n = 206, POC: n = 215	This study
Catchment C, Upper North Grain, S. Pennines*	53°26′31″N , 001°50′16″W	0.043			1592		21.7	16.4	blanket bog, severe erosion, 2019, DOC: n = 153, POC: n = 245	This study
Catchment Tr, Bleaklow, S. Pennines		0.0007		4.3				92.5	Bare, deep gullies, 2007	As reported by Billett (2010)
Catchment P, Snake Pass, S. Pennines	53°26′07″N , 001°51′54″W	0.005		7.9			13	1.9 - 3.4	blanket bog, *Eriophorum spp.*, 2008	As reported by Billett (2010)
Catchment WC, North slopes of Bleaklow, S. Pennines	53°28′37″N , 001°49′13″W	0.02		13.1			65.6	37.7	blanket bog, shrubs *Vaccinium spp.* and *Empetrum spp.*, 2008	As reported by Billett (2010)
Fleet Moss, Yorkshire Dales	54°14055″N, 2°12053″W	0.017	550 - 580		1997			340.9	blanket bog, 60 % bare, 2016 - 2017	Li et al. (2019)
Upper North Grain, S. Pennines*		0.38	490 - 541		1200		18.5	74	blanket bog, severe erosion, 2005-2006, n = 247	Pawson et al. (2008)
Cottage Hill Sike, N. Pennines*	54°41′N, 2°23′W	0.174	545 - 580	0 - 5	2012	5.8	51.5 – 63.4	2.4 - 3.0	98% blanket bog, relatively uneroded catchment, 2008-2009	Holden et al. (2012)
Nant y Brwyn, Migneint, Wales	55° 47′ N, 03°14′W	1	415 - 487		2200	5.6	19.3	0.9	peat dominated, 2006 - 2008	As reported by Billett et al. (2010)
Lady Clough, S. Pennines		1.33						44.8		Pawson (2008)
Auchencorth Moss, Scotland	55° 47′ N, 03° 14′W	3.4	249 - 300		1155	10	25.4	3.6	low-lying ombrotrophic peatland (85% peat), 2007 - 2008	Dinsmore et al. (2010)
Brocky Burn, N.E. Scotland		1.3	270 - 549		1164	7.5	16.9		Blanket bog with heather moorland	Dawson et al. (2002)
Trout Beck, Moor House NNR, N. Pennines*	54° 65′ N, 2°45W	11.4	450 - 893		1982	5.3	10.3 - 25.2	7–22.4 ±86%	ca. 90% peat, 1993 – 2005	Worrall et al. (2009)

* Reported to have included water sampling during storms

4.4. The role of pipes in fluvial carbon budgets

This study investigated the pipe-to-stream transfer of fluvial carbon of a pipe outlet issuing onto a streambank with signs of headward retreat (head pipe), as opposed to pipes issuing onto straight streambank sections (edge pipes). Regensburg et al. (2021) reported that head pipes at UNG contributed a greater proportion of water to stream flow than edge pipes. Excavation of a small part of two head pipes (H1 and H2 – both with discharge monitored in Regensburg et al. (2021)), after monitoring had stopped, showed contrasting features, with pipe H1 being a narrow but straight 4 cm wide vertical crack of ~60 cm deep running perpendicular to the gully edge with its roof ~20 cm below the peat surface, whereas pipe H2 drained a ~8 cm wide confined circular tube-like channel perpendicular to the gully edge with its bottom on a seemingly fixed horizon about 45 cm under the peat surface. Cunliffe et al. (2013) found the pipe-peat interface in blanket bog to be more permeable in the roof section than on the lateral sides or under it, but only studied one perennial pipe at ~0.3 m depth. However, the occurrence of biaxial and triaxial anisotropy of hydraulic conductivity in near-surface peat and in peat around pipes in blanket bog may be an important control for the variation in the routing of the pipe segments we found at greater depths. This heterogeneity of hydraulic conductivity across the peat profile might control the spatial reach over which pipes can drain water, and during wetter conditions, would provide good hydrological connectivity of the pipe network explaining runoff excess beyond the surface topographic catchment area. Dividing the total proportion of flow over the weir of DJF-2019 by DJF-2018 (as provided in Table 2) results in ratios of 1.5, 1.72 and 1.04 for catchment C, catchment T and pipe H1 respectively, suggesting a longer duration of hydrological connectivity during wetter periods in catchment T than in catchment C, where fewer pipes were observed. However, the duration of flow in pipe H1 was similar in both winters, and pipe H1 was active for longer in winter 2018 than catchment T, but the opposite was observed in the same period in 2019, suggesting wetter conditions on the surface do not necessarily result in better hydrological connectivity in pipe networks. These discrepancies highlight the complexity of the mechanisms that control flow in pipe networks, and these factors that control flow need further research.

Earlier studies on piping in the northern Pennines of UK showed that pipes undulate through the peat profile (Holden, 2004) and they may transport carbon of very different ages (Billett et al., 2012). Those studies were mainly conducted at pipes in landscapes with wide and shallow gullying, whereas UNG has pipes situated in close proximity to deep eroded gullies, which may not allow for long, uninterrupted branching pipe networks. In addition, sediment budgets of UNG have shown gully bank erosion to play a significant role in stream DOC and POC flux (Evans et al., 2006b). The absorbance ratios were consistent between pipe H1 and catchment T, indicating the humic fraction of their effluent had the same composition and originated from the same source. This suggests that DOC concentrations at pipe H1 may have been influenced from water infiltrating near the gully banks, via surface runoff entering the pipe via vent holes, or infiltration close to the pipe outlet, as hypothesised by Daniels et al. (2008). The larger POC flux from pipe H1 compared to other pipes in more intact blanket bog, could be indicative of internal erosion processes working differently in more degraded peats, but comparisons on piping processes between sites of differing degradation status do not exist and thus further research on this is recommended.

In this study, examining differences at the catchment outlet following pipe blocking was the main objective, and pipe H1 was monitored to assess some of the processes involved. Pipe H1 produced fewer discharge than pipe H2 (Regensburg et al., 2021), therefore fluxes for DOC and POC from pipe H1 may not be representative of all head pipes in the catchment. However, if we use the fluxes observed for pipe H1 as a maximum flux for pipes and scale up the DOC_{254} flux for pipe H1 to all 24 head pipes identified in catchment T by Regensburg et al. (2020), we can estimate that pipes contribute up to 56 % of the stream DOC_{254} flux of catchment T, providing the DOC is not precipitated or transformed on route to the stream network (Palmer et al., 2016). If we scale up the POC flux from pipe H1 to the 24 head pipes, the contribution of POC from pipes would potentially exceed the observed POC flux of catchment T for 2019, suggesting that the majority of the POC exported from pipes in this system are deposited at the pipe outlet, or trapped in the vegetated parts of the streambed (Evans and Warburton, 2005; Evans et al., 2006b; Shuttleworth et al., 2015), or transformed to DOC within the stream (Palmer et al., 2016). The temporary storage of POC at the pipe outlet and in the vegetated streambed are likely to control the episodic nature of POC export observed at the catchment outlet, with POC potentially being re-mobilised during large storms. While pipe H1 had a flow peak of ~0.86 L s^{-1} (Regensburg et al., 2021), the data on DOC and POC flux from pipe H1 presented here were mostly collected at discharges smaller than 0.5 L s^{-1} (Figure S4), and it may be that more data at larger discharges would alter the relationships presented in Table 1, particularly affecting sediment dynamics in the gully system. Pipe surveys conducted by Regensburg et al. (2020) showed that southwest and west-facing gully walls hosted ~40% of all identified pipe outlets in UNG. The aspect of gully walls is considered an important control on sediment distribution on the gully wall (Shuttleworth et al., 2017). Aspect may therefore be an important factor in the distribution of particulates deposited at pipe outlets. In a degraded system such as UNG, the episodic POC export by pipes may enhance DOC availability in the stream throughout the year via biodegradation and photodegradation (Worrall and Moody, 2014). However, the residence time and fate of particulate sediment deposited at the pipe outlet is unknown, but could play an important role in carbon budgets of piped peatland systems, and thus needs further research. Higher POC fluxes in catchment C may be the result of gully walls collapsing rather than the addition of POC from pipes, as it had considerably fewer (head) pipes than catchment T. In summary, the uncertainty in flux estimates of DOC and POC is indicative of pipes being a more complex component in the carbon cycling of degraded blanket peats than thought previously. Pipe networks in UNG are not just a passive pathway for water and carbon flow through the catchment, but form an active contributor, with loads that are quite different to those at stream outlets.

5. Conclusions

Impeding pipeflow by blocking the outlets of pipes in a degraded blanket bog catchment has been shown to be ineffective in moderating the export of fluvial carbon at both the pipe outlet and catchment scale. Therefore, it is not recommended that peatland practitioners undertake blocking of pipe outlets on gully walls as part of restoration measures to reduce aquatic carbon loads. We suggest that this recommendation applies to other piped environments where sediment load reductions are sought because hydraulic pressures near pipe outlets may lead to new outlets forming in the vicinity of the blocked outlet, as observed in our study. Further research could test the role of pipe blocking at several points further upslope away from pipe outlets as this may have a different impact on aquatic carbon flux. However, that would be more laborious and require mapping of subsurface pipe networks. In the case of highly degraded peatlands, we hypothesise that upslope pipe blocking (rather than pipe outlet blocking) is more likely to be effective in reducing POC fluxes than DOC fluxes since we found that pipe and stream water DOC had very similar composition, indicating a similar source. Despite the fact that impeding pipeflow by pipe outlet blocking at UNG was not successful in reducing water colour or DOC and POC concentrations and fluxes, we showed pipe erosion from a head pipe in UNG to be as high as the highest rates observed in a large ephemeral pipe in more intact blanket bog. The frequency of head pipes at UNG may form implications for peatland practitioners to consider when dealing with pipeflow and pipe erosion in the drainage network of degraded peatlands. We showed that fluvial carbon export by pipe outlets has a distinctive role in the fluvial carbon export of a degraded blanket bog system, and should therefore be included in future carbon budgets of blanket peatlands.

Data availability

The data for this paper will be made available on the University of Leeds data repository with a published DoI to be released once the paper is accepted.

References

Anderson, A.E., Weiler, M., Alila, Y., Hudson, R.O., 2009. Dye staining and excavation of a lateral preferential flow network. Hydrology and Earth System Sciences, 13(6), 935-944.

Anderson, M.G., Burt, T.P., 1982. Throughflow and pipe monitoring in the humid temperate environment. In: R. Bryan, A. Yair (Eds.), Badland geomorphology and piping. Geo Books, Norwich, pp. 337-353.

Baillie, I.C., 1975. Piping as an erosion process in the uplands of Sarawak. Journal of Tropical Geography, 41, 9-15.

Ball, D.F., 1964. Loss-On-Ignition As An Estimate Of Organic Matter And Organic Carbon In Non-Calcareous Soils. Journal of Soil Science, 15(1), 84-92.

Bernatek-Jakiel, A., Poesen, J., 2018. Subsurface erosion by soil piping: significance and research needs. Earth-Science Reviews, 185, 1107-1128.

Billett, M.F., Charman, D.J., Clark, J.M., Evans, C.D., Evans, M.G., Ostle, N.J., Worrall, F., Burden, A., Dinsmore, K.J., Jones, T., McNamara, N.P., Parry, L., Rowson, J.G., Rose, R., 2010. Carbon balance of UK peatlands: current state of knowledge and future research challenges. Climate Research, 45, 13-29.

Billett, M.F., Dinsmore, K.J., Smart, R.P., Garnett, M.H., Holden, J., Chapman, P., Baird, A.J., Grayson, R., Stott, A.W., 2012. Variable source and age of different forms of carbon released from natural peatland pipes. Journal of Geophysical Research: Biogeosciences, 117(G2), Artn G02003.

Bonn, A., Holden, J., Parnell, M., Worrall, F., Chapman, P.J., C.D., E., Termansen, M., Beharry-Borg, N., Acreman, M.C., Rowe, E., Emmett, B., Tsuchiya, A., 2010. Ecosystem services of peat – Phase 1, DEFRA.

Bower, M.M., 1961. The Distribution of Erosion in Blanket Peat Bogs in the Pennines. Transactions and Papers (Institute of British Geographers), 29, 17-30.

Brown, L.E., Aspray, K.L., Ledger, M.E., Mainstone, C., Palmer, S.M., Wilkes, M., Holden, J., 2019. Sediment deposition from eroding peatlands alters headwater invertebrate biodiversity. Global Change Biology, 25(2), 602-619.

Chapman, P.J., McDonald, A.T., Tyson, R., Palmer, S.M., Mitchell, G., Irvine, B., 2010. Changes in water colour between 1986 and 2006 in the headwaters of the River Nidd, Yorkshire, UK. Biogeochemistry, 101(1), 281-294.

Chapman, P.J., Reynolds, B., Wheater, H.S., 1993. Hydrochemical changes along stormflow pathways in a small moorland headwater catchment in Mid-Wales, UK. Journal of Hydrology, 151(2), 241-265.

Chico, G., Clutterbuck, B., Clough, J., Lindsay, R., Midgley, N.G., Labadz, J.C., 2020. Geo-hydromorphological assessment of Europe's southernmost blanket bogs. Earth Surface Processes and Landforms, 45(12), 2747-2760.

Clark, J.M., Lane, S.N., Chapman, P.J., Adamson, J.K., 2007. Export of dissolved organic carbon from an upland peatland during storm events: Implications for flux estimates. Journal of Hydrology, 347(3), 438-447.

Clay, G.D., Evans, M.G., 2017. Ten-year meteorological record for an upland research catchment near the summit of Snake Pass in the Peak District, UK. Weather, 72(8), 242-249.

Cunliffe, A.M., Baird, A.J., Holden, J., 2013. Hydrological hotspots in blanket peatlands: Spatial variation in peat permeability around a natural soil pipe. Water Resources Research, 49(9), 5342-5354.

Daniels, S.M., Agnew, C.T., Allott, T.E.H., Evans, M.G., 2008. Water table variability and runoff generation in an eroded peatland, South Pennines, UK. Journal of Hydrology, 361(1), 214-226.

Dawson, J.J.C., Billett, M.F., Neal, C., Hill, S., 2002. A comparison of particulate, dissolved and gaseous carbon in two contrasting upland streams in the UK. Journal of Hydrology, 257(1), 226-246.

de Wit, H., Ledesma, J., Futter, M., 2016. Aquatic DOC export from subarctic Atlantic blanket bog in Norway is controlled by seasalt deposition, temperature and precipitation. Biogeochemistry, 127.

Dinsmore, K.J., Billett, M.F., Skiba, U.M., Rees, R.M., Drewer, J., Helfter, C., 2010. Role of the aquatic pathway in the carbon and greenhouse gas budgets of a peatland catchment. 16(10), 2750-2762.

Evans, C.D., Chapman, P.J., Clark, J.M., Monteith, D.T., Cresser, M.S., 2006a. Alternative explanations for rising dissolved organic carbon export from organic soils. Global Change Biology, 12(11), 2044-2053.

Evans, C.D., Renou-Wilson, F., Strack, M., 2016. The role of waterborne carbon in the greenhouse gas balance of drained and re-wetted peatlands. Aquatic Sciences, 78(3), 573-590.

Evans, M., Lindsay, J., 2010. Impact of gully erosion on carbon sequestration in blanket peatlands. Climate Research, 45, 31-41.

Evans, M., Warburton, J., 2005. Sediment budget for an eroding peat-moorland catchment in northern England. Earth Surface Processes and Landforms, 30(5), 557-577.

Evans, M., Warburton, J., 2007. Geomorphology of upland peat : erosion, form and landscape change. Blackwell, Oxford.

Evans, M., Warburton, J., Yang, J., 2006b. Eroding blanket peat catchments: Global and local implications of upland organic sediment budgets. Geomorphology, 79(1), 45-57.

Faulkner, H., 2013. Badlands in marl lithologies: A field guide to soil dispersion, subsurface erosion and piping-origin gullies. Catena, 106, 42-53.

Fearing, D.A., Banks, J., Guyetand, S., Monfort Eroles, C., Jefferson, B., Wilson, D., Hillis, P., Campbell, A.T., Parsons, S.A., 2004. Combination of ferric and MIEX® for the treatment of a humic rich water. Water Research, 38(10), 2551-2558.

Gaffney, P.P.J., Hancock, M.H., Taggart, M.A., Andersen, R., 2021. Catchment water quality in the year preceding and immediately following restoration of a drained afforested blanket bog. Biogeochemistry, 153(3), 243-262.

González, E., Rochefort, L., 2018. Restoration of ombrotrophic bogs in the East of Canada. In: J.M.F.-G.a.F.J. Pérez (Ed.), Inventory, value and restoration of peatlands and mires: recent contributions.

Holden, J., 2004. Hydrological connectivity of soil pipes determined by ground-penetrating radar tracer detection. Earth Surface Processes and Landforms, 29(4), 437-442.

Holden, J., 2005a. Controls of soil pipe frequency in upland blanket peat. Journal of Geophysical Research: Earth Surface, 110, Artn F01002.

Holden, J., 2005b. Piping and woody plants in peatlands: Cause or effect? Water Resources Research, 41(6), n/a-n/a.

Holden, J., Smart, R.P., Dinsmore, K.J., Baird, A.J., Billett, M.F., Chapman, P.J., 2012. Natural pipes in blanket peatlands: major point sources for the release of carbon to the aquatic system. Global Change Biology, 18(12), 3568-3580.

Holden, J., Wallage, Z.E., Lane, S.N., McDonald, A.T., 2011. Water table dynamics in undisturbed, drained and restored blanket peat. Journal of Hydrology, 402(1), 103-114.

Hongve, D., Riise, G., Kristiansen, J.F., 2004. Increased colour and organic acid concentrations in Norwegian forest lakes and drinking water – a result of increased precipitation? Aquatic Sciences, 66(2), 231-238.

Jarvis, R.A., Bendelow, V.C., Bradley, R.I., Carroll, D.M., Furness, R.R., Kilgour, I.N.L., King, S.J., 1984. Soils and their use in northern England.

Jones, J.A.A., Richardson, J.M., Jacob, H.J., 1997. Factors controlling the distribution of piping in Britain: a reconnaissance. Geomorphology, 20(3-4), 289-306.

Labadz, J.C., Burt, T.P., Potter, A.W.R., 1991. Sediment yield and delivery in the blanket peat moorlands of the southern Pennines. Earth Surface Processes and Landforms, 16(3), 255-271.

Leifeld, J., Menichetti, L., 2018. The underappreciated potential of peatlands in global climate change mitigation strategies. Nature Communications, 9(1), 1071.

Li, C., Holden, J., Grayson, R., 2019. Sediment and fluvial particulate carbon flux from an eroding peatland catchment. Earth Surface Processes and Landforms.

Li, P., Holden, J., Irvine, B., Mu, X., 2017. Erosion of Northern Hemisphere blanket peatlands under 21st-century climate change. Geophysical Research Letters, 44(8), 3615-3623.

Marzolff, I., Ries, J., 2011. Piping as a process of gully erosion in small-format aerial photography. A short note. Cuadernos de investigación histórica, 37, 115-120.

MFFP, 2014. LiDAR (0.5 m x 0.5 m) and aerial imagery with 0.08 m ground resolution - dataset produced by BlueSky. Moors for the Future Partnership, Edale, UK.

Palmer, S.M., Evans, C.D., Chapman, P.J., Burden, A., Jones, T.G., Allott, T.E.H., Evans, M.G., Moody, C.S., Worrall, F., Holden, J., 2016. Sporadic hotspots for physico-chemical retention of aquatic organic carbon: from peatland headwater source to sea. Aquatic Sciences, 78(3), 491-504.

Pawson, R.R., 2008. Assessing the role of particulates in the fluvial organic carbon flux from eroding peatland systemsPhD thesis, University of Manchester, Manchester.

Pawson, R.R., Evans, M.G., Allott, T.E.H.A., 2012. Fluvial carbon flux from headwater peatland streams: significance of particulate carbon flux. Earth Surface Processes and Landforms, 37(11), 1203-1212.

Pawson, R.R., Lord, D.R., Evans, M.G., Allott, T.E.H., 2008. Fluvial organic carbon flux from an eroding peatland catchment, southern Pennines, UK. Hydrology and Earth System Sciences, 12(2), 625-634.

Peacock, M., Jones, T.G., Futter, M.N., Freeman, C., Gough, R., Baird, A.J., Green, S.M., Chapman, P.J., Holden, J., Evans, C.D., 2018. Peatland ditch blocking has no effect on dissolved organic matter (DOM) quality. Hydrological Processes, 32(26), 3891-3906.

Ramchunder, S.J., Brown, L.E., Holden, J., 2012. Catchment-scale peatland restoration benefits stream ecosystem biodiversity. Journal of Applied Ecology, 49(1), 182-191.

Rapson, G.L., Sykes, M.T., Lee, W.G., Hewitt, A.E., Agnew, A.D.Q., Wilson, J.B., 2006. Subalpine gully-head ribbon fens of the Lammerlaw and Lammermoor Ranges, Otago, New Zealand. New Zealand Journal of Botany, 44(4), 351-375.

Regensburg, T.H., Chapman, P.J., Pilkington, M.G., Chandler, D.M., Evans, M.G., Holden, J., 2020. Controls on the spatial distribution of natural pipe outlets in heavily degraded blanket peat. Geomorphology, 367, 107322.

Regensburg, T.H., Chapman, P.J., Pilkington, M.G., Chandler, D.M., Evans, M.G., Holden, J., 2021. Effects of pipe outlet blocking on hydrological functioning in a degraded blanket peatland. Hydrological Processes, 35(3), e14102.

Renou-Wilson, F., Moser, G., Fallon, D., Farrell, C.A., Müller, C., Wilson, D., 2019. Rewetting degraded peatlands for climate and biodiversity benefits: Results from two raised bogs. Ecological Engineering, 127, 547-560.

Rothwell, J.J., 2006. Fluvial export of heavy metals from contaminated and eroding peatlands, southern Pennines, UKPhD thesis, University of Manchester, Manchester.

Rothwell, J.J., Evans, M.G., Allott, T.E.H., 2007. Lead contamination of fluvial sediments in an eroding blanket peat catchment. Applied Geochemistry, 22(2), 446-459.

Rothwell, J.J., Robinson, S.G., Evans, M.G., Yang, J., Allott, T.E.H., 2005. Heavy metal release by peat erosion in the Peak District, southern Pennines, UK. Hydrological Processes, 19(15), 2973-2989.

Sayer, A.M., Walsh, R.P.D., Bidin, K., 2006. Pipeflow suspended sediment dynamics and their contribution to stream sediment budgets in small rainforest catchments, Sabah, Malaysia. Forest Ecology and Management, 224(1), 119-130.

Shuttleworth, E.L., Clay, G.D., Evans, M.G., Hutchinson, S.M., Rothwell, J.J., 2017. Contaminated sediment dynamics in peatland headwater catchments. Journal of Soils and Sediments, 17(11), 2637-2647.

Shuttleworth, E.L., Evans, M.G., Hutchinson, S.M., Rothwell, J.J., 2015. Peatland restoration: controls on sediment production and reductions in carbon and pollutant export. Earth Surface Processes and Landforms, 40(4), 459-472.

Shuttleworth, E.L., Evans, M.G., Pilkington, M., Spencer, T., Walker, J., Milledge, D., Allott, T.E.H., 2019. Restoration of blanket peat moorland delays stormflow from hillslopes and reduces peak discharge. Journal of Hydrology X, 2, 100006.

Smart, S.M., Henrys, P.A., Scott, W.A., Hall, J.R., Evans, C.D., Crowe, A., Rowe, E.C., Dragosits, U., Page, T., Whyatt, J.D., Sowerby, A., Clark, J.M., 2010. Impacts of pollution and climate change on ombrotrophic Sphagnum species in the UK: analysis of uncertainties in two empirical niche models. Climate Research, 45, 163-176.

Tipping, E., Rieuwerts, J., Pan, G., Ashmore, M.R., Lofts, S., Hill, M.T.R., Farago, M.E., Thornton, I., 2003. The solid–solution partitioning of heavy metals (Cu, Zn, Cd, Pb) in upland soils of England and Wales. Environmental Pollution, 125(2), 213-225.

Urban, N.R., Bayley, S.E., Eisenreich, S.J., 1989. Export of dissolved organic carbon and acidity from peatlands. Water Resources Research, 25(7), 1619-1628.

Valdeolivas, G., Serrano, B., Sánchez, C., 2018. Recovery of the Bernallán bog in the upper basin of the River Miera. In: J.M.F.-G.a.F.J. Pérez (Ed.), Inventory, value and restoration of peatlands and mires: recent contributions.

Valdivia-Garcia, M., Weir, P., Frogbrook, Z., Graham, D.W., Werner, D., 2016. Climatic, Geographic and Operational Determinants of Trihalomethanes (THMs) in Drinking Water Systems. Scientific Reports, 6(1), 35027.

Van der Wal, R., Bonn, A., Monteith, D., Reed, M., Blackstock, K., Hanley, N., Thompson, D., Evans, M., Alonso, I., Allott, T., Armitage, H., Beharry, N., Glass, J.J.S., McMorrow, J., Ross, L., Pakeman, R., Perry, S., Tinch, D., 2011. Mountains, Moorlands and Heaths, UNEP-WCMN, Cambridge.

Verachtert, E., Maetens, W., Van Den Eeckhaut, M., Poesen, J., Deckers, J., 2011. Soil loss rates due to piping erosion. Earth Surface Processes and Landforms, 36(13), 1715-1725.

Walling, D.E., Webb, B.W., 1985. Estimating the discharge of contaminants to coastal waters by rivers: Some cautionary comments. Marine Pollution Bulletin, 16(12), 488-492.

Ward, S.E., Bardgett, R.D., McNamara, N.P., Adamson, J.K., Ostle, N.J., 2007. Long-term consequences of grazing and burning on northern peatland carbon dynamics. Ecosystems, 10(7), 1069-1083.

Watts, C.D., Naden, P.S., Machell, J., Banks, J., 2001. Long term variation in water colour from Yorkshire catchments. Science of The Total Environment, 278(1-3), 57-72.

Williamson, C.E., Overholt, E.P., Pilla, R.M., Leach, T.H., Brentrup, J.A., Knoll, L.B., Mette, E.M., Moeller, R.E., 2015. Ecological consequences of long-term browning in lakes. Scientific reports, 5, 18666-18666.

Wilson, G., 2011. Understanding soil-pipe flow and its role in ephemeral gully erosion. Hydrological Processes, 25(15), 2354-2364.

Wolverson Cope, F., 1998. Geology Explained in the Peak District. Scarthin Books, Derbyshire.

Worrall, F., Burt, T., Shedden, R., 2003. Long term records of riverine dissolved organic matter. Biogeochemistry, 64(2), 165-178.

Worrall, F., Burt, T.P., Rowson, J.G., Warburton, J., Adamson, J.K., 2009. The multi-annual carbon budget of a peat-covered catchment. Science of the Total Environment, 407(13), 4084-4094.

Worrall, F., Moody, C.S., 2014. Modeling the rate of turnover of DOC and particulate organic carbon in a UK, peat-hosted stream: Including diurnal cycling in short-residence time systems. Journal of Geophysical Research: Biogeosciences, 119(10), 1934-1946.

Xu, J., Morris, P.J., Liu, J., Holden, J., 2018. Hotspots of peatland-derived potable water use identified by global analysis. Nature Sustainability, 1(5), 246-253.

Xu, X., Wilson, G.V., Zheng, F., Tang, Q., 2020. The role of soil pipe and pipeflow in headcut migration processes in loessic soils. Earth Surface Processes and Landforms, 45(8), 1749-1763.

Yeloff, D.E., Labadz, J.C., Hunt, C.O., 2006. Causes of degradation and erosion of a blanket mire in the southern Pennines, UK. Mires and Peat, 1(Artn. 4), 1-18.